Journal of Nuclear Medicine, published on February 3, 2022 as doi:10.2967/jnumed.121.263004

Short-term colony stimulating factor-1 receptor inhibition-induced repopulation after stroke assessed by longitudinal 18F-DPA-714 PET imaging

Cristina Barca[1,2]*, Amanda J Kiliaan[3], Lydia Wachsmuth[4], Claudia Foray[1,2], Sven Hermann[1], Cornelius Faber[4], Michael Schäfers[1,5], Maximilian Wiesmann[3], Bastian Zinnhardt[1,2,5,6#] and Andreas H Jacobs[1,2,7#]*

[1]European Institute for Molecular Imaging, University of Münster, Münster, Germany

[2]PET Imaging in Drug Design and Development (PET3D)

[3]Department of Medical Imaging, Anatomy, Radboud University Medical Center, Nijmegen, The Netherlands

[4]Translational Research Imaging Center, University Hospital Münster, Münster, Germany

[5]Department of Nuclear Medicine, University Hospital Münster, Münster Germany

[6]Biomarkers & Translational Technologies (BTT), Pharma Research & Early Development (pRED), F. Hoffmann-La Roche Ltd., Basel, Switzerland

[7]Department of Geriatrics and Neurology, Johanniter Hospital, Bonn, Germany

[#]*Equal contribution*

*Corresponding authors: Andreas H. Jacobs (PI) and Cristina Barca (PhD)

European Institute for Molecular Imaging

University of Münster, Waldeyerstrasse 15

D-48149 Münster

e-mail addresses: ahjacobs@uni-muenster.de

cristina.barca@uni-muenster.de

Word count: 5049

Short title: Short-term CSF-1R inhibition in stroke

KEYWORDS

Colony stimulating factor-1 receptor, microglia, stroke, 18F-DPA-714, repopulation

ABSTRACT

Studies on colony stimulating factor-1 receptor (CSF-1R) inhibition-induced microglia depletion indicated that inhibitor withdrawal allowed the renewal of the microglial compartment via repopulation and resolved the inflammatory imbalance. Therefore, we investigated for the first time the effects of microglia repopulation on inflammation and functional outcomes in an ischemic mouse model using translocator protein (TSPO) positron emission tomography (PET)- computed tomography (CT)/ magnetic resonance (MR) imaging, *ex vivo* characterization and behavioral tests. **Methods**: N=8/group C57BL/6 mice underwent a 30 minutes transient middle cerebral artery occlusion. The treatment group received CSF-1R inhibitor 1200 ppm PLX5622 chow (Plexxikon Inc.) from days 3 to 7 to induce microglia/macrophages depletion, and went back to control diet to allow microglia repopulation. Mice underwent T_2w-MR imaging on day 1 and 18F-DPA-714 (TSPO) PET-CT on days 7, 14, 21 and 30 post ischemia. Percentage of injected tracer dose (%ID/mL) within the infarct, contralateral striatum and spleen were assessed. Behavioral tests were performed to assess motor function recovery. Brains were harvested at days 14 and 35 post ischemia for *ex vivo* analyses (immunoreactivity, rt-qPCR) of microglia/macrophages-related markers. **Results**: Repopulation significantly increased 18F-DPA-714 tracer uptake within the infarct on days 14 ($p < 0.001$) and 21 ($p = 0.002$) post ischemia. On day 14, the Iba-1$^+$ cell population showed significantly higher expression of TSPO, CSF-1R and CD68, in line with microglia repopulation. Gene expression analyses on day 14 indicated a significant increase in microglia-related markers (*csf-1r*, *aif1*, *p2ry12*) with repopulation while peripheral cell recruitment-related gene expression decreased (*cx3cr1*, *ccr2*), indicative of peripheral recruitment during CSF-1R inhibition. Similarly, uncorrected spleen tracer uptake was significantly higher on day 7 post ischemia with treatment ($p = 0.001$) and decreased after drug withdrawal. PLX5622-treated mice walked longer distance ($p < 0.001$) and faster ($p = 0.009$), and showed stronger forelimbs strength ($p < 0.001$) than control mice on day 14. **Conclusion**: This study highlights the potential of 18F-DPA-714 PET-CT imaging to track microglia/macrophages repopulation after short-term CSF-1R inhibition in stroke.

INTRODUCTION

Microglia play a major role in the stroke-induced neuroinflammatory response, as part of the early pro-inflammatory and later restorative processes (*1*). Microglia survival and proliferation are dependent upon signalling through the colony-stimulating factor 1 receptor (CSF-1R) (*2*). Administration of the CSF-1R inhibitor PLX5622 progressively leads to the almost complete microglia depletion after one week of treatment in wild type mice (*3*). Microglial depletion in acute/subacute ischemia (1-3 days) was associated to increased immune cell infiltration and aggravated brain inflammation (*4*,*5*). Inhibitor withdrawal triggers microglia repopulation, indicated by microglia proliferation and increased activity. Besides, long-lasting treatment effects were observed on other cell population (*6*). Recently, we demonstrated that CSF-1R inhibition-induced microglia/macrophages depletion could be tracked using 18F-DPA-714 radiotracer targeting the translocator protein (TSPO) (*7*): TSPO-dependent neuroinflammation was significantly decreased within the first weeks after stroke, although long-term CSF-1R inhibition was associated with poor disease outcome. Therefore, PLX5622 represents an attractive microglia/macrophages-targeting pharmacological tool allowing modulation of the inflammatory environment after stroke. However, microglia repopulation has yet to be investigated.

The therapeutic effect of short-term CSF-1R inhibition has been scarcely investigated but showed promising applications. In a neuronal injury mouse model, renewal of the microglial compartment after short-term CSF-1R inhibition reduced lesion-induced inflammatory markers, resolved the active phenotype of microglial cells and reversed behavioral impairment (*3*). Therefore, short-term PLX5622 treatment represents an opportunity to renew the cellular compartment and reprogram microglial activity to reduce ischemia-associated inflammation.

In this study, we aimed to longitudinally investigate the effects of microglial repopulation in a stroke mouse model. We investigated the therapy effect of microglia repopulation on stroke outcomes by inhibiting CSF-1R between days 3 to 7 post ischemia. Few studies in stroke models investigated how microglial cells affected

outcomes after CSF-1R inhibition (*4*,*5*,*8*). Results indicated that absence of microglia within the first days post stroke worsened disease outcomes, including increased brain injury, enhanced excitotoxicity and brain inflammation. Therefore, we aimed (i) to leverage the phagocytic activity on infiltrating immune cells and cell debris within the first days post ischemia (*4*); (ii) to reduce microglia-related excitotoxicity; (iii) to renew the microglial compartment and (iv) to take advantage of the repopulation process on lesion-associated inflammation at the peak of TSPO-dependent inflammation reported between days 10-14 post ischemia (*9*–*11*).

To investigate the kinetics of immune cell activation, we performed longitudinal positron emission tomography (PET) using the TSPO radiotracer 18F-DPA-714 as a marker for neuroinflammation, together with computed tomography (CT) and magnetic resonance imaging (MRI). Imaging data were cross-correlated with protein and gene expression profiles of microglia/macrophages and inflammation-related markers using immunohistochemistry and real time-qPCR. Besides, we studied the therapeutic effect on motor functions using a set of behavioral tests.

We hypothesized that subacute PLX5622 treatment may induce immunomodulatory effects by triggering microglia repopulation, ultimately showing positive effect on stroke outcomes. The repopulation process, indicated by an increased TSPO-PET signal, may non-invasively be detected by 18F-DPA-714 PET-MR imaging.

MATERIALS AND METHODS

Study Approval

All experiments were conducted in accordance with the German Law on the Care and Use of Laboratory Animals and approved by the Landesamt für Natur, Umwelt und Verbraucherschutz of North Rhine-Westphalia and according to the ARRIVE 2.0 guidelines (https://www.nc3rs.org.uk/arrive-guidelines).

Study

3-4 months old male C57BL6/J mice (N = 32) were provided by the local animal facility. They were housed under standard 12:12 hours light:dark cycles with free access to food and water. All mice underwent a 30 minutes (min) transient middle cerebral artery occlusion (tMCAo) (day 0) and were randomized into either control or PLX5622-treated group by an external person. All mice underwent T_2w-MR imaging on day 1. The treatment group received 1200 ppm PLX5622 chow from days 3 to 7 post ischemia (Figure 1). Experimenters were blind to group assignment.

Exclusion criteria were: (i) lack of reperfusion (< 50% baseline CBF recovery) assessed by laser Doppler, (ii) infarct exceeding striatal and cortical regions, and (iii) extreme weight loss (> 20% of the initial body weight). The drop-out rate was 8%.

N = 8/group were used for *in vivo* PET imaging on days 7, 14, 21 and 30 post ischemia. The same animals were used for behavioral assessment prior and after surgery. They were sacrificed at day 35 post ischemia to obtain late invasive data. An extra group of n = 8/group were added to characterize the 14-day time point as indicated in Supplementary Table 1.

On the last day of the experiment, mice were sacrificed by transcardial perfusion with phosphate-buffered saline (PBS). Brains reserved for immunoreactivity were fixed with 4% PFA in PBS while the others kept for real-time (rt) qPCR were flash-frozen in nitrogen and stored at -80°C.

Surgery

Stroke was induced by intra-luminal suture method as previously described (*12*). Briefly, mice were anesthetized with 5% isoflurane/O2 (Forene, Abbott, Germany) after intraperitoneal injection of buprenorphine (0.03 mg/kg bodyweight) and maintained at 2.5% v/v isoflurane/O2 on a heating pad during the entire procedure.

A 7-0 silicon rubber-coated monofilament (diameter with coating 0.19 ± 0.01 mm) (Doccol Corporation, USA) was inserted into the right internal carotid artery to block the MCA origin. After 30 min, the monofilament was removed to allow reperfusion. Mice received Buprenorphine (0.1 mg/kg bodyweight) and were placed under the infrared heating lamp until full recovery. Successful MCA occlusion and reperfusion were assessed measuring the cerebral blood flow by laser Doppler flowmetry (Periflux 5000, Perimed, Sweden).

Treatment

PLX5622 was provided by Plexxikon Inc. (Berkeley, USA), formulated in AIN-76A standard chow by Research Diets Inc. at 1200 ppm chow (USA) and stored at 4°C until use. Both control and PLX5622-enriched diets were provided ad libitum as described in Figure 1. Bodyweight was reported as an index of food intake (Supplementary Figure 1).

18F-DPA-714 PET-CT Imaging

18F-DPA-714(TSPO)-PET imaging was carried out on days 7, 14, 21 and 30 post ischemia using a high-resolution small animal PET scanner (32 module quadHIDAC, Oxford Positron Systems Ltd.) with uniform spatial resolution of < 1 mm (FWHM) over a cylindrical field-of-view (165 mm diameter, 280 mm axial length) (*13*).

Radiotracer was prepared as previously described with a >99% radiochemical purity (*14*). Once anaesthetized, mice received 12.9 ± 2.2 MBq via tail vein (specific activity: 40-80 GBq/µmol). Animals were kept anaesthetized in a warmed environment for 45 min. The scan was acquired from 45-65 min post injection. PET data were reconstructed using one-pass list mode expectation maximization algorithm with resolution recovery

(*13*). Images were only corrected for activity decay. After the PET scan, the animal bed was transferred into a CT scanner (Inveon, Siemens Medical Solutions, Knoxville, TN, USA) with a spatial resolution of 86 µm. PET-CT images were co-registered using a landmark approach.

MR Imaging

T_2 weighted-MR imaging (T_2w-MRI) was performed on day 1 to delineate the infarct. After anaesthesia (5% isoflurane/air, Forene, Abbott, Wiesbaden, Germany), mice were positioned on a heated MRI cradle and fixed by bite and ear bars. Animals were continuously supplied with 2 % isoflurane/air until the end of the experiment. Respiration and body temperature (37.0 ± 0.5°C) were constantly monitored. A small sheet prepared from 1% v/v agar-water solution was directly placed on the animal head to reduce susceptibility artifacts and covered with parafilm (Merck KGaA, Darmstadt, Germany). Two different systems were used:

With the first system, the cradle was manually positioned in the center of the 9.4 T small animal MRI scanner (Biospec 94/20, Bruker Biospin GmbH, Ettlingen, Germany). All images were processed and generated using Paravision 5.1 (Bruker Biospin MRI, Ettlingen, Germany). T_2-weighted images were acquired with a fast spin-echo sequence (RARE) (Repetition Time (TR) = 7700 ms, effective Echo Time (TE) = 100 ms, rare factor = 30, Field Of View (FOV) = 2 cm x 2 cm, slice thickness = 0.5 mm, interslice distance = 0 cm, number of slices = 20, matrix = 192x192, number of averages = 8).

With the second system, a T2 FSE 2D sequence was acquired in a 1T nanoScan PET/MRI scanner equipped with a MH20 coil (Mediso Medical Imaging Systems, resolution: 0.27x0.27x0.9 mm).

Behavioral Tests

Open field, grip test, rotarod and pole test were performed to assess the treatment effect on motor functions recovery as previously described (*7*,*15*). The four behavioral tests were carried out the week prior to

surgery and on days 14 and 35, as indicated in Figure 1. Protocols are described in Supplementary Material & Methods.

Image Analysis

PET-CT images from the same mouse were manually co-registered with T_2w-MR images acquired on day 1. An atlas was adjusted to anatomical landmarks, following bone structure and ventricles, and manually corrected. The infarct was delineated using a thresholding approach previously described (*11*). Radiotracer uptake was assessed within the T_2w-MRI-defined infarct, the atlas-based contralateral striatum and manually delineated spleen. Radiotracer uptake was reported in percentage of injected dose per millilitre (%ID/mL) in both regions, and the infarct-to-contralateral striatum was calculated.

Immunoreactivity

Brains were fixed in 4% PFA, embedded in paraffin and cut in 5 µm coronal sections. Immunohistochemistry and immunofluorescence were performed as previously described (*7*). Iba-1, GFAP and TSPO expression level was visualized and quantified by immunoreactivity. Moreover, TSPO cellular source was assessed with Iba-1/TSPO, CSF-1R/TSPO, CD68/TSPO and GFAP/TSPO co-staining. Primary and secondary antibodies are reported in Supplementary Table 2.

Images were obtained using a confocal microscope (Nikon Eclipse NI-E, Nikon, Japan) and images were displayed with ImageJ software.

RT-qPCR

RT-qPCR was performed from snap-frozen half-brain tissues as previously described (*7*). The forward and reverse primer sequences were reported in Supplementary Table 3. Relative gene expression was assessed using the ΔΔCt method, with Gapdh (Biomol Gmbh, Germany) as a housekeeping gene.

Statistical Analysis

All the statistical analyses were performed using SigmaPlot Version 13.0 (Systat Software, San Jose, CA). The datasets were tested for normal distribution and equal variance.

The sample size was determined based on effect size (p = 0.05, power: 1-β = 0.80), mortality rates and previous stroke studies (*7*,*15*), where we investigated the therapeutic effect of dietary approaches on brain inflammation assessed by 18F-DPA-714 PET imaging. Intra-individual 18F-DPA-714 PET imaging data, behavioral test, gene expression and immunoreactivity datasets were analysed by repeated measures ANOVA followed by Sidak's post hoc test for multiple comparisons, unless stated otherwise. All data were expressed as mean ± standard error of the mean (SEM).

RESULTS

Both experimental groups showed similar infarct size on day 1 ($p = 0.59$) (Supplementary Figure 2).

We performed longitudinal 18F-DPA-714 PET-CT imaging to assess repopulation process (Figure 2A). ANOVA analysis indicated significant increased tracer uptake within the infarct compared to the contralateral striatum over time (Supplementary Figure 3). Two-way RM ANOVA analysis indicated a significant effect of time ($p < 0.001$), treatment ($p = 0.007$) and time*treatment ($p = 0.009$) on tracer uptake within the infarct (Figure 2B). In the control group, intra-individual comparison indicated that the mean uptake decreased at day 30 compared to days 14 ($p = 0.024$) and 21 ($p = 0.022$). In PLX5622-treated mice, tracer uptake increased from day 7 to day 14 ($p < 0.001$) and remained elevated by day 21 ($p < 0.001$). Later, radiotracer uptake significantly decreased at day 30 compared to days 14 ($p < 0.001$) and 21 ($p < 0.001$) post ischemia. Treatment effect was observed on days 14 and 21 post ischemia: PLX5622-treated mice showed increased 18F-DPA-714 tracer uptake within the infarct at both days 14 ($p < 0.001$) and 21 ($p = 0.002$) compared to control mice. Similarly, the infarct-to-contralateral striatum ratio indicated a significant effect of both time ($p = 0.008$) and treatment ($p = 0.043$) (Figure 2C). Treatment effects were observed on days 14 and 21: PLX5622-treated mice showed higher mean ratios compared to control mice on both days 14 ($p = 0.043$) and 21 ($p = 0.041$). 18F-DPA-714 PET imaging data on days 14 and 30 were further cross-validated by immunohistochemistry (Supplementary Figure 4).

Temporal dynamic of 18F-DPA-714 uptake within the spleen indicated treatment effect ($p = 0.027$) on days 7 and 30 post ischemia, where PLX5622-treated mice showed higher tracer uptake compared to control mice (Supplementary Figure 5).

We determined the number of Iba-1$^+$ cells (microglia/macrophages) within the infarct, at the periphery of the infarct and in the contralateral striatum for both experimental groups on both days 14 and 35 (Supplementary Figure 6). On day 14, qualitative assessment of Iba-1$^+$ cell morphology indicated higher ramification in control than

PLX5622-treated mice at both the periphery and contralateral side. At day 35, PLX5622-treated mice showed significantly decreased percentage of Iba-1-positive area within the infarct compared to control mice ($p < 0.001$).

We further characterized the Iba-1-positive cell population within the infarct by immunofluorescence (Figure 3). Both control and PLX5622-treated mice showed a mixed population of Iba-1$^+$TSPO$^+$ and Iba-1$^+$TSPO$^-$ cells within the infarct while TSPO expression was higher in PLX5622-treated mice, in line with the 18F-DPA-714 PET data acquired at day 14. However, PLX5622-treated mice showed a higher number of Iba-1$^+$CSF-1R$^+$ and Iba-1$^+$CD68$^+$ (activated myeloid cells) cells within the infarct than control mice, in line with the repopulation process.

We investigated the potential treatment effect of short-term CSF-1R inhibition on (GFAP-positive) astrocytes at days 14 and 35 post ischemia (Supplementary Figure7). At day 14, PLX5622-treated mice showed significantly higher percentage of GFAP-positive area compared to control mice within the infarct ($p = 0.014$) and the contralateral striatum ($p < 0.001$). Sustained effect was observed in the contralateral striatum at day 35. However, no colocalization between GFAP and TSPO was observed, indicating that astrocytes were not contributing to 18F-DPA-714 PET signal.

Gene expression of microglia/macrophages-related markers was assessed at day 14 (Figure 4). PLX5622-treated mice showed significantly higher *csf-1r* ($p = 0.001$) and *aif1* (also known as Iba-1) ($p = 0.008$) expression compared to control mice in the contralateral hemisphere. Good correlation between *csf-1r* and *aif1* was observed (correlation: $R^2 = 0.86$, $p = 0.34$, Supplementary Figure 8). Moreover, PLX5622-treated mice showed a significant increase in *p2ry12* expression, a marker for anti-inflammatory activated microglial cells, compared to control mice in both infarct ($p = 0.043$) and contralateral ($p = 0.01$) hemispheres. On the other hand, PLX5622 treatment significantly decreased *cx3cr1* (fractalkine receptor constitutively present on microglia/macrophages, $p = 0.009$) in the contralateral hemisphere and *mrc1* (mannose receptor expressed by CNS macrophages, $p = 0.009$) expression in the infarct hemisphere. Expression of *ccr2*, mostly found on monocytes, was significantly increased in the contralateral hemisphere ($p = 0.002$) but decreased in the ipsilateral hemisphere ($p = 0.048$) (Figure 4). No

treatment effect was observed on *trem2* expression, a marker of phagocytic activity ($p > 0.05$). Gene expression analysis on day 35 post ischemia indicated long-lasting treatment effects on *aif1*, *cx3cr1* and *trem2* gene expression (Supplementary Figure 9).

Behavioral tests indicated that PLX5622-treated mice travelled a longer distance ($p < 0.001$) and faster at day 14 ($p = 0.009$) compared to control mice in the OF (Figure 5A-B). Treatment effect was also observed on the latency to fall in the rotarod test, where PLX5622-treated mice had increased latency to fall compared to control mice ($p < 0.005$) at both days 14 and 35 post ischemia (Figure 5C). No treatment effect was observed on motor functions/coordination assessed with the pole test ($p = 0.47$) (Figure 5D). Additionally, forelimb strength was significantly better in PLX5622-treated mice at day 14 ($p = 0.038$) (Figure 5E). No correlation between behavioral parameters and tracer uptake on day 14 was observed ($R^2_{OF} = 0.01$ ($p = 0.34$), $R^2_{rotarod} = 0.1$ ($p = 0.44$), $R^2_{grip} = 0.55$ ($p = 0.11$)).

DISCUSSION

In this study, we investigated for the first time the immunomodulatory effect of CSF-1R inhibition-induced microglia repopulation in the subacute ischemic period using *in vivo* multimodal imaging. We demonstrated that 18F-DPA-714 PET imaging serves as a sensitive biomarker to the glial repopulation. In both experimental groups, the Iba-1$^+$ cell population was one of the major sources of TSPO expression while astrocytes did not express TSPO. After one week of repopulation, the Iba-1$^+$ cells displayed significantly higher expression of TSPO, CSF-1R and CD68 expression, with altered morphology at the periphery of the infarct and in the contralateral striatum, indicative of an activated state. Gene expression analysis indicated a treatment effect on microglia/macrophages-related gene expression in line with the repopulation process. *Csf-1r* and *p2ry12* expression increased during repopulation and increased *csf-1r* expression positively correlated with higher *aif1* levels, indicative of microglia/macrophages repopulation with a potential switch towards an anti-inflammatory state. Gene expression of peripheral cell recruitment markers was altered during repopulation on day 14, indicating increased recruitment of peripheral immune cells during microglia depletion while repopulation may reverse the effect. This hypothesis was supported by the significantly increased spleen tracer uptake after depletion, as a sign of increased systemic inflammation, and subsequent decreased during the repopulation process in PLX5622-treated mice. Additionally, functional outcomes were improved with repopulation: PLX5622-treated mice showed faster motor recovery at day 14 post ischemia including longer distance travelled and higher velocity in three out of the four selected tests, suggesting that repopulation could rescue motor functions. Altogether, this study highlighted the renewal of the microglia/macrophages compartment with CSF-1R inhibitor as a possible new immunomodulatory treatment paradigm after stroke that could be track by 18F-DPA-714 PET imaging.

The translocator protein (TSPO) is a transmembrane protein found at the outer mitochondrial membrane involved in metabolic functions (*16*). TSPO expression is markedly increased in glial cells (microglia, astrocytes)

and/or peripheral immune cells (monocytes, lymphocytes) under inflammatory conditions, which makes it a suitable biomarker of inflammation and/or activated immune cells (*17*).

18F-DPA-714 PET has been used in many translational studies to track TSPO-dependent inflammatory reaction after stroke (*7*,*9*,*10*,*15*). Many studies have confirmed that the dynamics of 18F-DPA-714 tracer correlate with $CD11b^{+}TSPO^{+}$/$Iba\text{-}1^{+}TSPO^{+}$ cell number, supporting its use to *in vivo* track microglia/macrophages-targeting immunomodulatory therapies. However, TSPO PET imaging alone may not be suitable to determine a treatment time window or assess the therapy outcome. The main reason is that TSPO has multiple cellular sources, which show a continuum of differentiated states going from pro- to anti-inflammatory phenotypes. Therefore, interpretation of TSPO-PET signal benefits from dedicated ex vivo analyses for characterization of the inflammatory response. Nevertheless, in vivo PET imaging may support the determination of therapeutic windows of immunomodulatory compounds by allowing intra-individual follow-up and visualization of disease relevant molecular processes.

In this study, we support the use of 18F-DPA-714 to track microglia/macrophages repopulation after CSF-1R inhibitor withdrawal. We observed increased TSPO-PET signal within the infarct on days 14 and 21, cross-validated by immunohistochemistry/fluorescence. Dual labelling indicated $Iba\text{-}1^{+}$ cells as one of the major cellular sources of TSPO expression while astrocytes did not show any TSPO expression, indicating that tracer uptake was mostly modulated by the microglia/macrophages activity/dynamic.

Based on previously published data (*7*), a partial depletion can be expected. According to previous studies, CSF-1R inhibition triggers increased peripheral immune cell infiltration (*4*,*5*). Altogether, it could explain the similar tracer uptake at the end of the treatment period (day 7). Additionally, a recent report indicated that the repopulation kinetic depends on the extent of microglia depletion (*18*). Partial depletion resulted in slower repopulation rate compared to full depletion. Microglial numbers did not recover within the first week following partial depletion while numbers exceed by +160% after complete depletion (*19*). This effect may partly explain

the significantly increased TSPO expression at days 14 and 21 post ischemia. Expression of many microglia/macrophages-related markers was increased at day 14 post ischemia in the infarct and/or contralateral hemisphere, in line with the repopulation process.

CSF-1R/CSF-1 axis regulates developmental functions such as proliferation and survival of microglia (*20*). Here, our data indicated a global significant increase of *csf-1r* and CSF-1R expression in PLX5622-treated mice at day 14 post ischemia compared to control animals, as a sign of microglia/macrophages repopulation after inhibitor withdrawal. Additionally, P2ry12 is a specific marker for microglia cells that is downregulated in pro-inflammatory environment and upregulated with exposure to anti-inflammatory stimuli, turning into an interesting biomarker for anti-inflammatory microglia (*21*). Our data indicated a flare effect on *p2ry12* expression at day 14 post ischemia, suggesting that repopulation may trigger a beneficial anti-inflammatory state favouring tissue recovery. Further characterization indicated the presence of a highly activated Iba-1^{+} CD68^{+} cell population in PLX5622-treated mice triggered by the repopulation process, as previously reported (*18*).

While gene expression analysis indicated increased microglia/macrophages related genes such as *csf-1r*, *p2ry12* and *aif1*, peripheral immune cells-related genes such as *ccr2* and *cx3cr1* were significantly downregulated during repopulation within the infarct. Therefore, we hypothesized that subacute CSF-1R inhibition triggered peripheral recruitment and repopulation reversed the process. Supporting this hypothesis, we observed a significantly increased 18F-DPA-714 tracer uptake in the spleen during depletion, suggesting an increased adaptive/peripheral inflammatory response with treatment. However, tracer uptake in peripheral organs must be corrected for metabolites for exact interpretation. Still, we supported previous studies showing that CSF-1R inhibition could trigger the engraftment of peripherally derived macrophages into parenchyma and that repopulation reduced gene expression involved in monocyte chemoattraction and leukocyte transmigration (*3*,*4*,*22*).

In our model of mild cerebral ischemia, repopulation accelerated motor function recovery as shown in three of the four behavioral tests. Behavioral parameters did not correlate with TSPO-PET signal assessed at day 14. We hypothesized that changes in immune cell population could partly explain the faster recovery in PLX5622-treated mice, including renewal of the microglia compartment and/or increased anti-inflammatory central/peripheral cell population within the infarct. Few studies reported that short-term depletion after brain lesion promoted functional recovery (*3*,*23*), correlating with changes in neuroprotective factors expression.

Late invasive data indicated that repopulation reduced number of Iba-1^{+} cells within the infarct, decreased *cx3cr1* expression and *trem2*-dependent phagocytic activity at day 35 post ischemia while astrogliosis was increased. This result suggests that repopulation may resolve stroke-induced microglia/macrophages phenotype.

CONCLUSION

We demonstrated that microglia/macrophages repopulation following short-term CSF-1R inhibition could be assessed by *in vivo* 18F-DPA-714 PET-CT/MR imaging. Repopulation induced changes in glial morphology, phenotype, gene expression and cell recruitment, with signs of improved functional recovery. Further evaluations should identify which cell subpopulations are responsive to CSF-1R inhibition and repopulation. Overall, we propose a promising immunotherapy paradigm targeting microglia activity potentiating stroke recovery.

DISCLOSURE

The authors declare no conflict of interest.

ACKNOWLEDGEMENTS

This work was partly funded by the Horizon 2020 Programme under grant agreement n° 675417 (PET3D), the 'Cells-in-Motion' Cluster of Excellence (DFG EXC1003 - CiM), Münster, Germany, the Interdisciplinary Center for Clinical Research (IZKF core unit PIX), Münster, Germany and the Walter Worch Stiftung, Germany.

The authors thank Dirk Reinhardt, Sarah Köster, Christine Bätza, Roman Priebe, Stefanie Bouma, Irmgard Hoppe, Christa Möllmann, Nina Knubel and Florian Breuer for their excellent technical support.

KEY POINTS

a. PET imaging is a valuable tool to assess immunomodulatory effect of microglia-targeting therapy.

b. Brain repopulation in inflammatory environment showed therapeutic effects on stroke outcomes.

c. 18F-DPA-714 PET imaging allows tracking repopulation process after short-term CSF-1R inhibition.

REFERENCES

1. Jiang C, Wu W, Deng Y, Ge J. Modulators of microglia activation and polarization in ischemic stroke (Review). *Mol Med Rep*. 2020;21:2006-2018.

2. Elmore MRP, Najafi AR, Koike MA, et al. Colony-stimulating factor 1 receptor signaling is necessary for microglia viability, unmasking a microglia progenitor cell in the adult brain. *Neuron*. 2014;82:380-397.

3. Rice RA, Pham J, Lee RJ, Najafi AR, West BL, Green KN. Microglial repopulation resolves inflammation and promotes brain recovery after injury. *Glia*. 2017;65:931-944.

4. Otxoa-de-Amezaga A, Miró-Mur F, Pedragosa J, et al. Microglial cell loss after ischemic stroke favors brain neutrophil accumulation. *Acta Neuropathol*. 2019;137:321-341.

5. Jin W-N, Shi SX-Y, Li Z, et al. Depletion of microglia exacerbates postischemic inflammation and brain injury. *J Cereb Blood Flow Metab*. 2017;37:2224-2236.

6. Lei F, Cui N, Zhou C, Chodosh J, Vavvas DG, Paschalis EI. CSF1R inhibition by a small-molecule inhibitor is not microglia specific; affecting hematopoiesis and the function of macrophages. *Proc Natl Acad Sci*. 2020;117:23336-23338.

7. Barca C, Kiliaan AJ, Foray C, et al. A longitudinal PET/MR imaging study of colony stimulating factor-1 receptor-mediated microglia depletion in experimental stroke. *J Nucl Med*. 2021;In press.

8. Szalay G, Martinecz B, Lénárt N, et al. Microglia protect against brain injury and their selective elimination dysregulates neuronal network activity after stroke. *Nat Commun*. 2016;7:11499.

9. Martín A, Boisgard R, Thézé B, et al. Evaluation of the PBR/TSPO radioligand 18F-DPA-714 in a rat model of focal cerebral ischemia. *J Cereb Blood Flow Metab*. 2010;30:230-241.

10. Zinnhardt B, Viel T, Wachsmuth L, et al. Multimodal imaging reveals temporal and spatial microglia and

matrix metalloproteinase activity after experimental stroke. *J Cereb Blood Flow Metab*. 2015;35:1711-1721.

11. Barca C, Foray C, Hermann S, et al. Characterization of the inflammatory post-ischemic tissue by full volumetric analysis of a multimodal imaging dataset. *Neuroimage*. 2020;222:117217.

12. Engel O, Kolodziej S, Dirnagl U, Prinz V. Modeling stroke in mice - middle cerebral artery occlusion with the filament model. *J Vis Exp*. 2011;47:2423.

13. Schäfers KP, Reader AJ, Kriens M, Knoess C, Schober O, Schäfers M. Performance evaluation of the 32-module quadHIDAC small-animal PET scanner. *J Nucl Med*. 2005;46:996-1004.

14. James ML, Fulton RR, Vercoullie J, et al. DPA-714, a new translocator protein-specific ligand: synthesis, radiofluorination, and pharmacologic characterization. *J Nucl Med*. 2008;49:814-822.

15. Barca C, Wiesmann M, Calahorra J, et al. Impact of hydroxytyrosol on stroke: tracking therapy response on neuroinflammation and cerebrovascular parameters using PET-MR imaging and on functional outcomes. *Theranostics*. 2021;11:4030-4049.

16. Veenman L, Gavish M. The role of 18 kDa mitochondrial translocator protein (TSPO) in programmed cell death, and effects of steroids on TSPO expression. *Curr Mol Med*. 2012;12:398-412.

17. Varrone A, Lammertsma AA. Imaging of neuroinflammation: TSPO and beyond. *Clin Transl Imaging*. 2015;3:389-390.

18. Najafi AR, Crapser J, Jiang S, et al. A limited capacity for microglial repopulation in the adult brain. *Glia*. 2018;66:2385-2396.

19. Elmore MRP, Lee RJ, West BL, Green KN. Characterizing newly repopulated microglia in the adult mouse: impacts on animal behavior, cell morphology, and neuroinflammation. Langmann T, ed. *PLoS One*.

2015;10.

20. Stanley ER, Chitu V. CSF-1 receptor signaling in myeloid cells. *Cold Spring Harb Perspect Biol*. 2014;6.

21. Villa A, Klein B, Janssen B, et al. Identification of new molecular targets for PET imaging of the microglial anti-inflammatory activation state. *Theranostics*. 2018;8:5400-5418.

22. Cronk JC, Filiano AJ, Louveau A, et al. Peripherally derived macrophages can engraft the brain independent of irradiation and maintain an identity distinct from microglia. *J Exp Med*. 2018;215:1627-1647.

23. Henry RJ, Ritzel RM, Barrett JP, et al. Microglial depletion with CSF1R inhibitor during chronic phase of experimental traumatic brain injury reduces neurodegeneration and neurological deficits. *J Neurosci*. 2020;40:2960-2974.

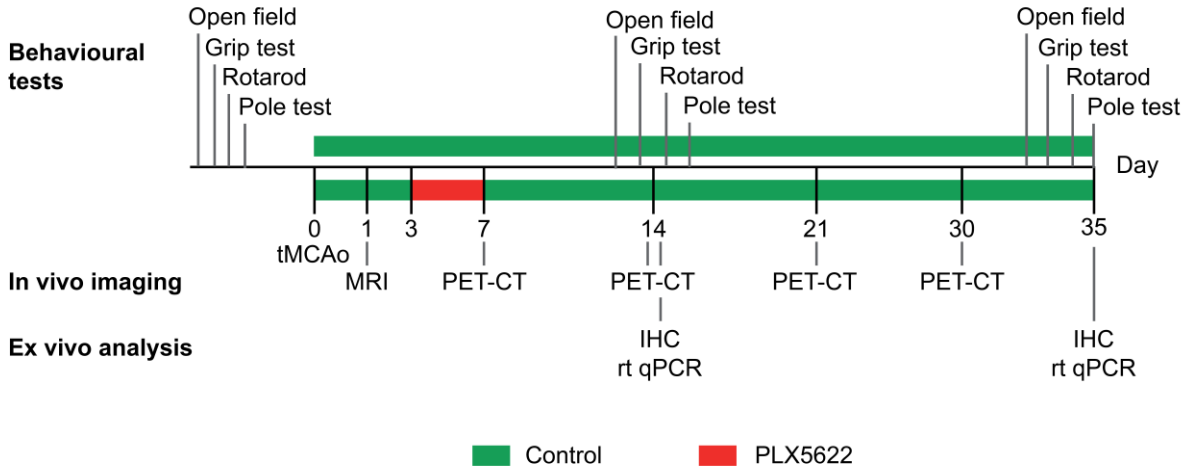

Figure 1. Study design.

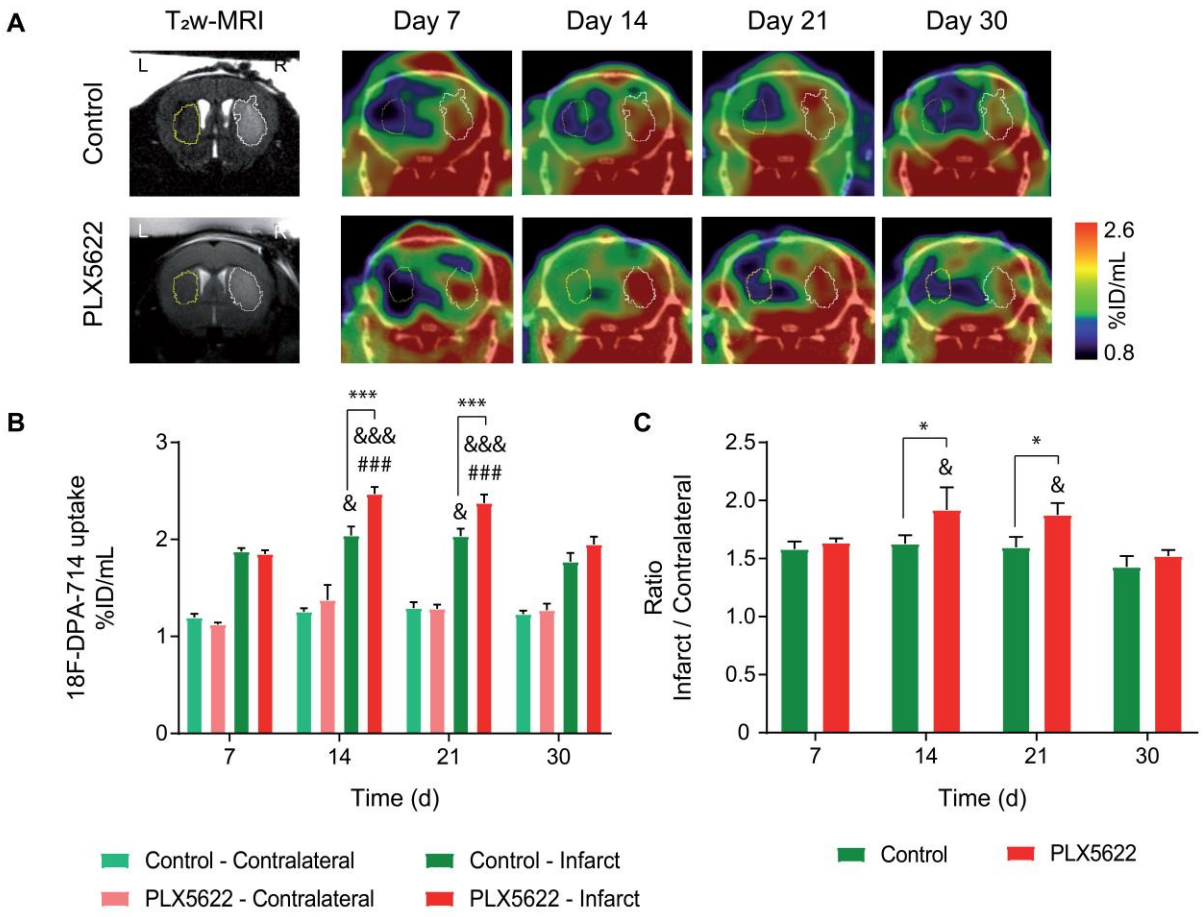

Figure 2. 18F-DPA-714 PET imaging. (A) Representative 18F-DPA-714 PET-CT images and corresponding T_2w-MR image. Quantification of (B) the mean 18F-DPA-714 uptake (%ID/mL) within the infarct and contralateral striatum and (C) the infarct-to-contralateral ratio (*p < 0.05, **p < 0.01, ***p < 0.005, * vs. treatment, # vs. day 7, & vs. day 30).

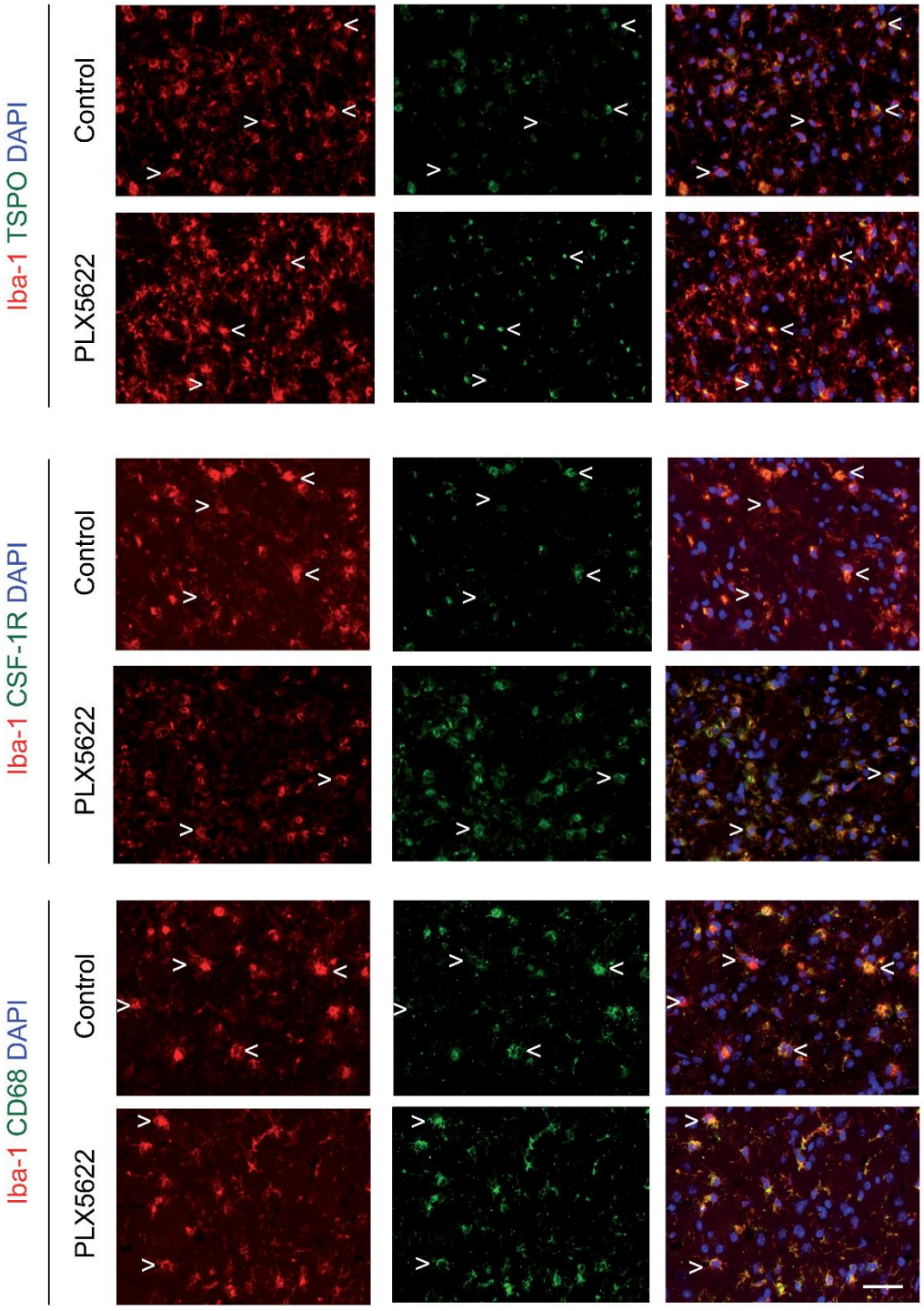

Figure 3. Characterization of the Iba-1-positive cell population at day 14 post ischemia. Immunofluorescent staining for TSPO, CSF-1R and CD68 in Iba-1-positive cell population in both control and PLX5622-treated mice at day 14 post ischemia. Scale bar: 20 µm (<: Iba-1$^+$ cell positive for the marker, >: Iba-1$^+$ cell negative for the marker).

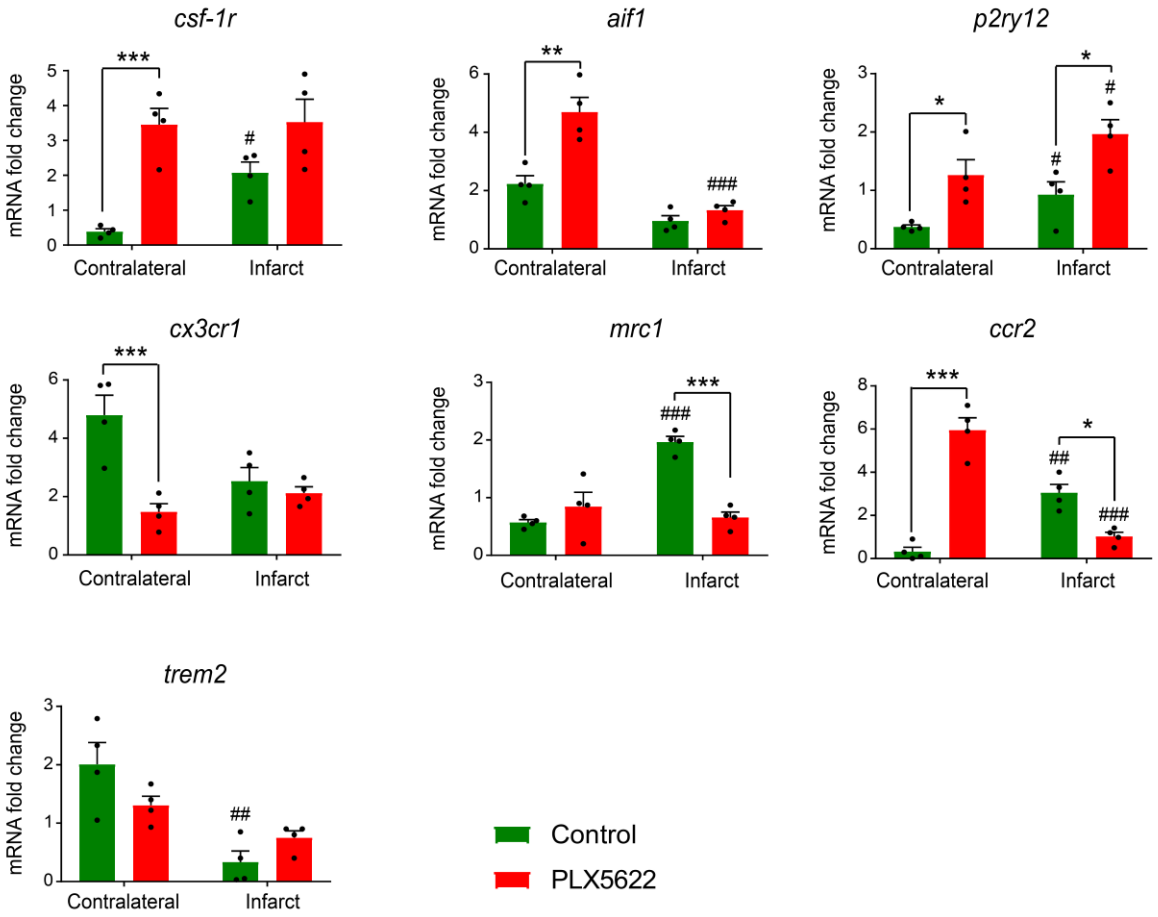

Figure 4. Gene expression of microglia/macrophages-related markers at day 14 post ischemia (*$p < 0.05$, **$p < 0.01$, ***$p < 0.005$, # vs contralateral).

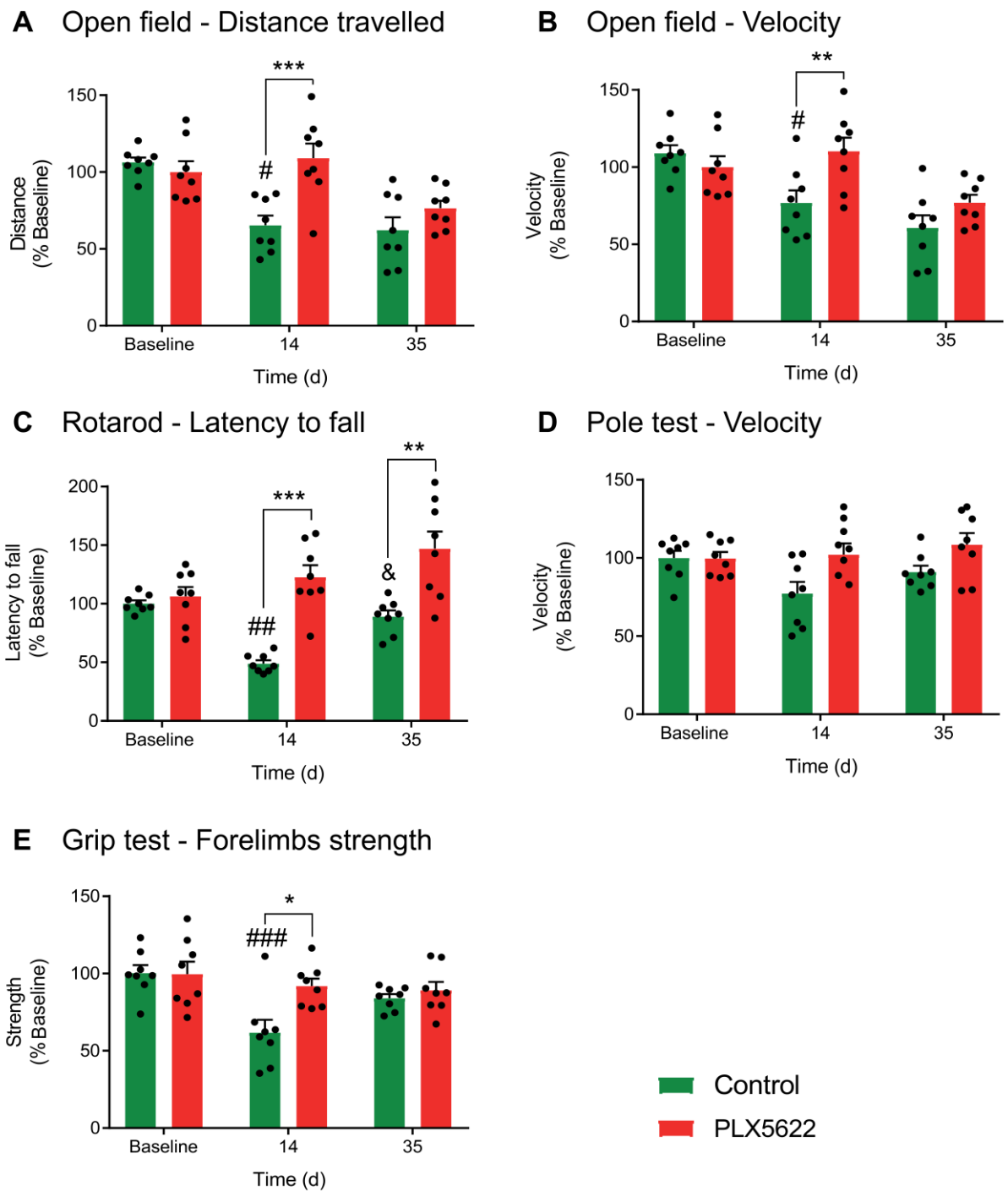

Figure 5. Behavioral tests. (A) Distance travelled and (B) speed in the open field, (C) latency to fall during the rotarod test, (D) velocity during the pole test and (E) forelimbs strength assessed with the grip test were assessed (*$p < 0.05$, **$p < 0.01$, ***$p > 0.005$, * vs. treatment, # vs. baseline, & vs. day 14).

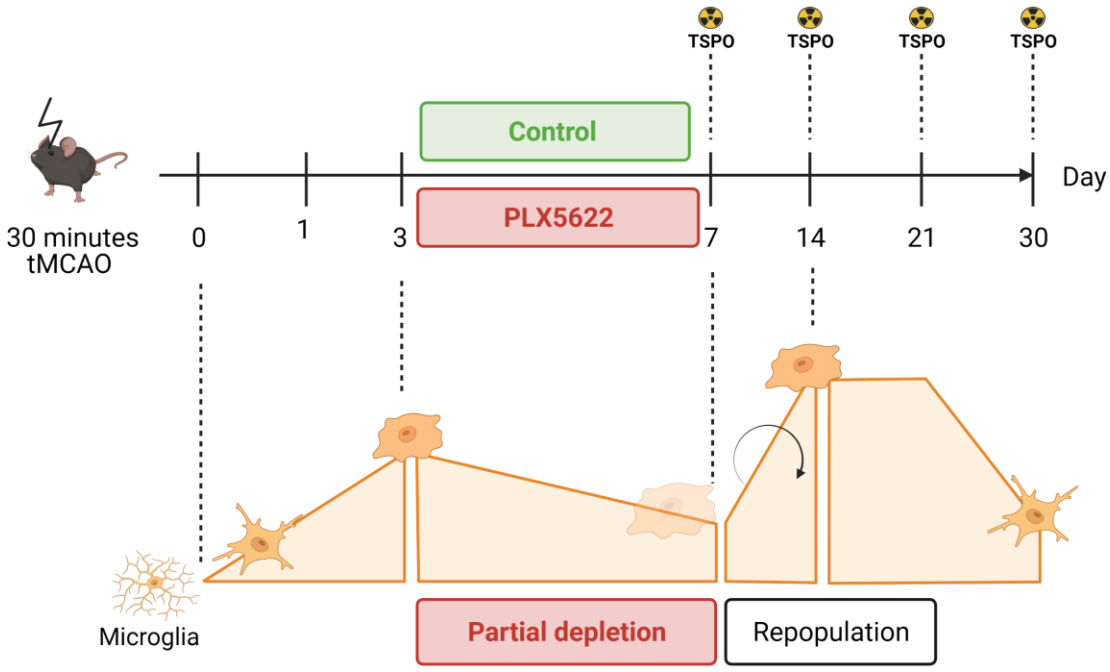

Graphical Abstract

Supplementary Materials & Methods

Behavioral tests

One week prior to behavioural tests, animals were brought to the institute and were daily handled for 10 minutes by the experimenter for acclimatization. Open field, grip test, rotarod and pole test were performed to evaluate the therapeutic effects of acute CSF-1R inhibition on motor function recovery. The four behavioural tests were carried out the week prior to surgery and at days 14 and 35 post ischemia.

Open field

The open field test is used to assess general locomotor activity level by recording free movements. A squared arena (40 x 40 x 25 cm^3) was placed in a quiet environment. Before the test, litter coming for the animal cage was spread in the arena to hide possible contaminating odours and let for 5 minutes. Once the litter has been removed, the mouse was placed in the middle of the maze and was free to move for 10 minutes. Locomotion was recorded using EthoVision XT15 (Noldus, Wageningen, The Netherlands) video tracking system attached to a pole placed above the arena. Distance travelled (cm), velocity (cm/s) and laterality (clockwise and counter-clockwise rotations of the center-nose axis) were measured.

Grip strength test

The grip test uses a grip strength meter (Grip-Strength Meter, 47200, Ugo Basile, Italy) to determine forelimbs muscle strength. The mouse was able to grasp the grip trapeze with the forepaws and was gently pulled away until the grasp was released. Each mouse was tested five times. The average of the peak force (in gf) was calculated from the last three trials.

Pole test

The pole test is a general test to assess motor functions. The mouse was placed head upward just below the top of a vertical pole (diameter: 2.5 cm; height: 60 cm) and then allowed to descend into their home

cage. The time needed to reach the floor was manually measured. Each mouse was tested five consecutive times, but only the last three trials are used for calculation.

Rotarod

The rotarod test (ITC LifeScience Inc., Woodland Hills, CA, USA) assesses motor coordination and balance. In this test, a mouse was placed on a rotating cylinder (3 cm in diameter) suspended 30 cm above the protected apparatus floor. The mouse was placed on the rod and left to acclimatise for 30 s. Then, the rotarod was turned on to accelerate in 300 s from 4 to 40 rpm. The trial is complete when the mouse fell down. The test was repeated five consecutive times. The time spent on the cylinder (in seconds) and the covered distance (in cm) were automatically recorded for each trial and reported as the latency to fall (in seconds). The averaged values were calculated from the last three trials.

Supplementary Table 1. Study design and animal number. Longitudinal PET imaging and behavioural tests were performed on n = 8 stroke mice per group (groups A & C). Those animal were sacrificed at the end of the study (day 35 post ischemia) for further *ex vivo* characterization. N= 4 mice/ group were used for immunoreactivity and n = 4 for gene expression analysis. Another n = 8 stroke mice per group were used to characterise the 14-day time point (groups B & D). Similarly, n = 4 mice/ group were used for immunoreactivity and n = 4 for gene expression analysis.

		In vivo			***Ex vivo***	
Group		**T_2w-MRI Day 1**	**18F-DPA-714 PET-CT**	**Behaviour**	**Day 14**	**Day 35**
Control	**A (n = 8)**	X	X	X		X
	B (n = 8)	X			X	
PLX5622	**C (n = 8)**	X	X	X		X
	D (n = 8)	X			X	

Supplementary Table 2. List of primary and secondary antibodies used for immunohistochemistry and immunofluorescence

Target	**Dilution**	**Species**	**ID**	**Provider**
Anti-TSPO	1:250	Rabbit	ab109497	Abcam
Recombinant Alexa Fluor 488 anti-TSPO	1:250	Rabbit	ab199779	Abcam
Anti-Iba-1	1:500	Rabbit	019-19741	Wako
Red fluorochrome (635)-conjugated Iba-1	1:500	Rabbit	013-26471	Wako
Anti-CSF-1R	1:250	Rabbit	SAB4500498	Merck
Anti-GFAP	1:500	Chicken	ab4675	Abcam
Anti-CD68	1:250	Rabbit	ab125212	Abcam
Biotin Anti-rabbit	1:800	Goat	B21078	Life Technologies
Biotin Anti-chicken	1:800	Goat	ab6876	Abcam
Alexa Fluor 488 anti-rabbit	1:1000	Goat	A-21206	Life Technologies
Alexa Fluor 555 anti-rabbit	1:1000	Goat	A-21432	Life Technologies
Alexa Fluor 488 anti-chicken	1:1000	Goat	A-11039	Life Technologies

Abbreviations: CSF-1R: *colony stimulating factor-1 receptor*; GFAP: *glial fibrillary acidic protein*; Iba-1: *ionized calcium binding adapter molecule-1*; TSPO: *translocator protein*; CD68: *cluster of differentiation 68*.

Supplementary Table 3. Primers for real-time qPCR.

Primer	Forward (FW)	Reverse (RV)
Csf-1r	gccatatacaggtacacattc	gtgccattaagaagtactgg
Cx3cr1	aacaccatgctgtcatattc	gtaagctactatgcttgctg
Ccr2	accacatgtgctaagaattg	ctggttttatgacaaggctc
P2ry12	taccctacagaaacactcaag	gctgaatctgaaggatatgag
Aif1	ttcatcctctctcttccatc	tcagcttttgaaatctcctc
Mrc1	aaatgatgagctgtggattg	ccatccttgcctttcataac
Trem2	tcatctcttttctgcacttc	tcataagtacatgacaccctc
Gapdh	ctggagaaacctgccaagta	tgttgctgtagccgtattca

Abbreviations: *Csf-1r*: Colony stimulating factor-1 receptor; *Cx3cr1*: C-X3-C chemokine receptor 1; *Ccr2*: C-C chemokine receptor 2; *P2ry12*: purinergic receptor P2Y12; *Aif1*: allograft inflammatory factor 1; *Mrc1*: mannose receptor C-type 1; *trem2*: Triggering receptor expressed on myeloid cells 2; *gapdh*: Glyceraldehyde 3-phosphate dehydrogenase.

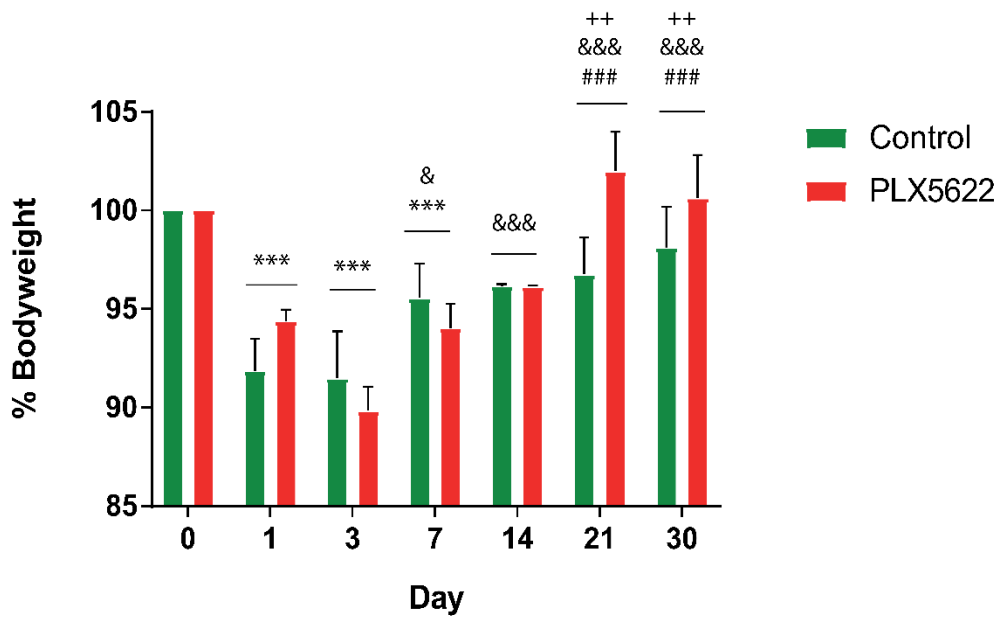

Supplementary Figure 1. Bodyweight. Two-way RM ANOVA indicated time effect ($p < 0.001$) but not treatment ($p = 0.57$) or time*treatment ($p = 0.084$) effect. In both groups, bodyweight significantly decreased within the first 3 days and then increased again (*$p < 0.05$, ** $p < 0.01$, *** $p < 0.005$, * *vs.* day 0, # *vs.* day 1, & *vs.* day 3, + *vs.* day 7).

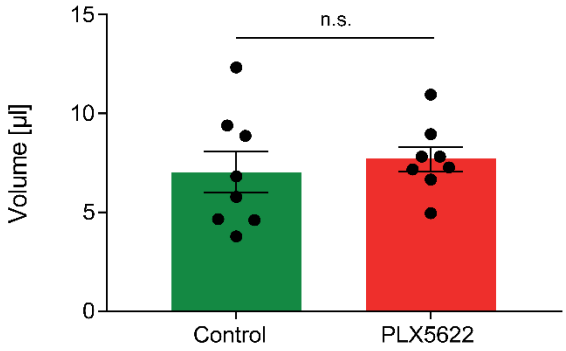

Supplementary Figure 2. T_2w-MRI-derived lesion on day 1 post ischemia. T-test indicated no significant difference between both experimental groups (control: 7.03 ± 2.76 µl, PLX5622: 7.70 ± 1.75 µl, $p = 0.22$).

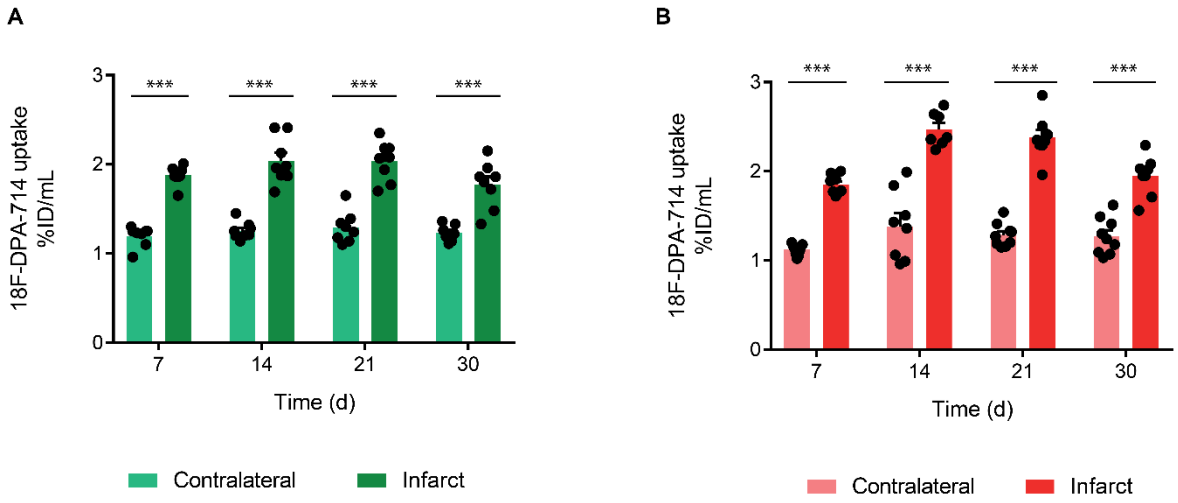

Supplementary Figure 3. 18F-DPA-714 tracer uptake (%ID/mL) of both (a) control and (b) PLX5622-treated mice within the infarct and the contralateral striatum. Two-way RM ANOVA indicated a significant effect of brain region in both groups ($p < 0.001$). Data are reported as mean ± SEM (*$p < 0.05$, ** $p < 0.01$, *** $p < 0.005$).

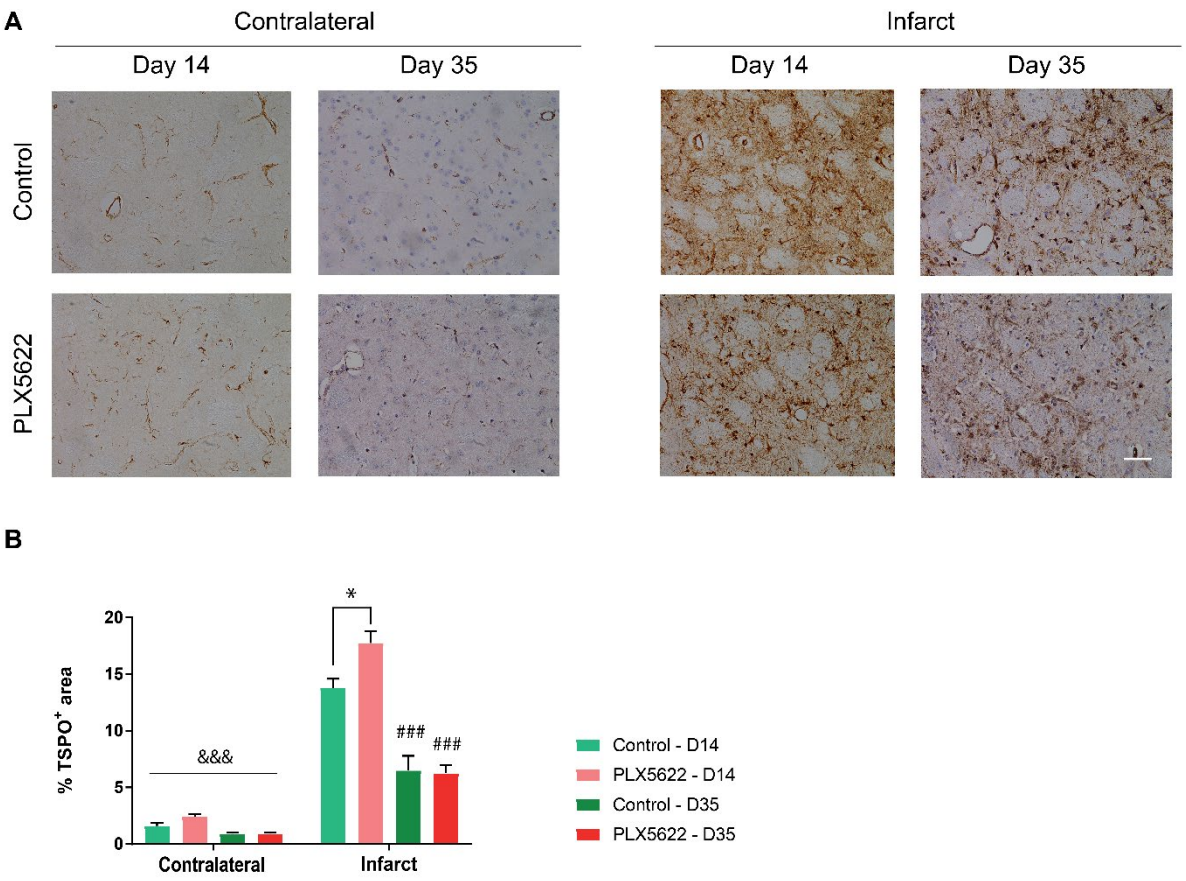

Supplementary Figure 4. 18F-DPA-714 PET imaging data were cross-validated by immunohistochemistry.

(A) Representative images of the anti-TSPO immunoreactivity showing TSPO-positive cells and vessels within the infarct and the contralateral tissues at both days 14 and 35 post ischemia for both control and PLX5622-treated mice. (B) Quantification of the images showed significant higher percentage of TSPO-positive area in PLX5622-treated mice compared to control mice within the infarct at day 14 ($p = 0.023$) while no difference was observed at day 35 post ischemia, cross-validating 18F-DPA-714 PET imaging data at both time points (*$p < 0.05$, ** $p < 0.01$, *** $p < 0.005$, * *vs.* treatment, # *vs.* time, & *vs.* infarct).

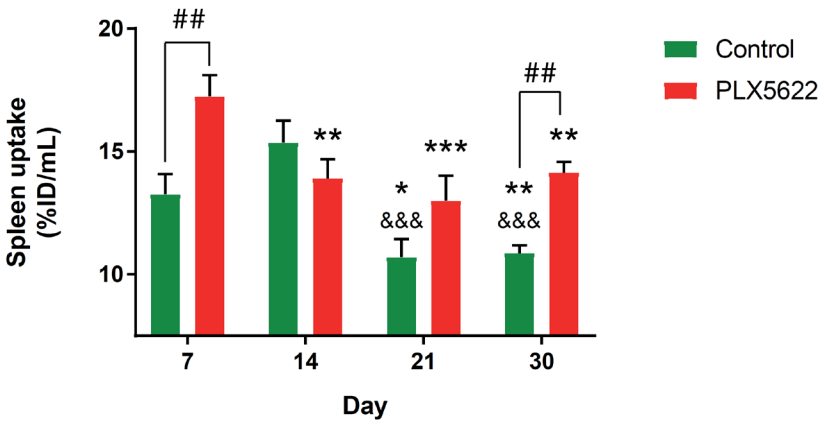

Supplementary Figure 5. 18F-DPA-714 tracer uptake within the spleen. The spleen was manually delineated on PET images co-registered with CT scans. The dataset passed the normality (p = 0.68) and equal variance (p = 0.42) tests. Statistical analysis indicated time (p < 0.001, power: 0.99), treatment (p = 0.027, power: 0.54) and time*treatment (p < 0.001) effects on spleen tracer uptake. Treatment effect was observed at days 7 and 30 post ischemia, where PLX5622-treated mice showed higher tracer uptake compared to control mice (*p < 0.05, ** p < 0.01, *** p < 0.005, * *vs.* day 7, & *vs.* day 14, # *vs.* treatment).

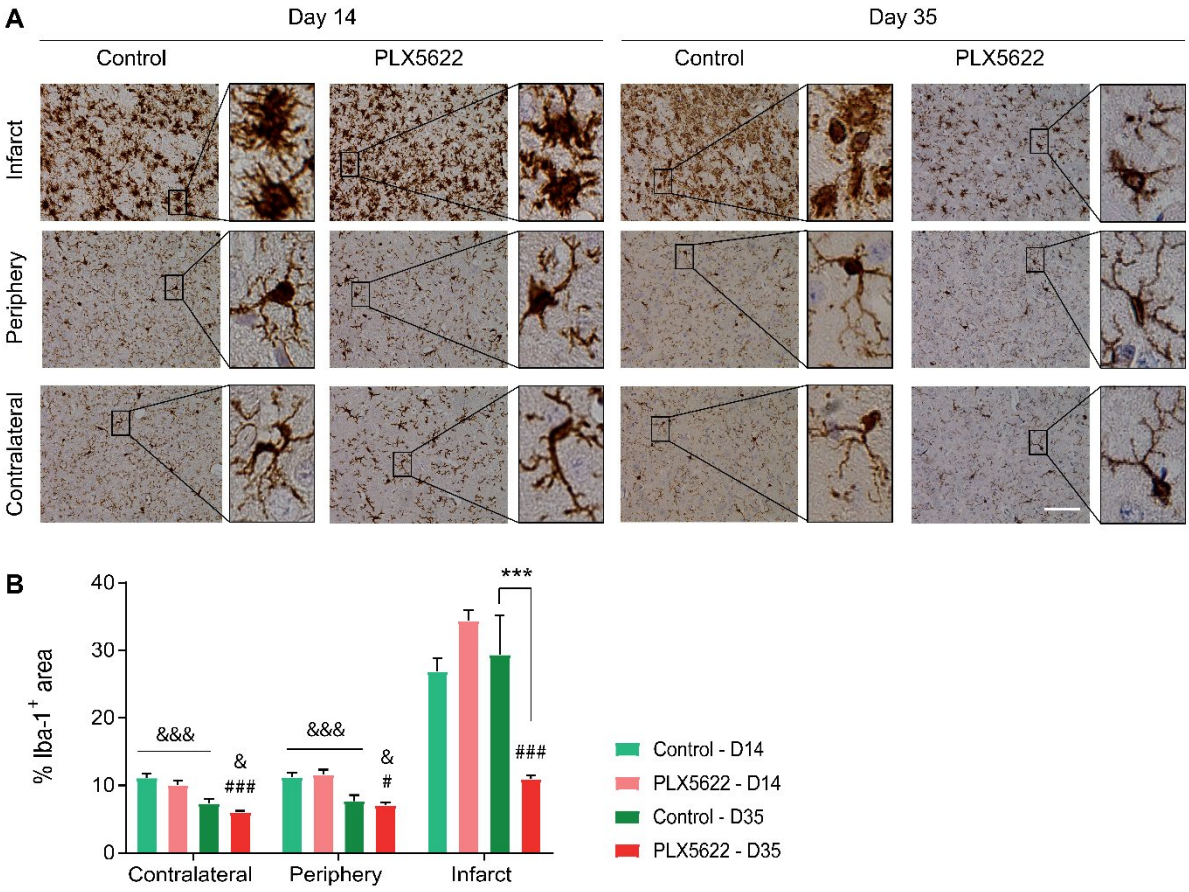

Supplementary Figure 6. Iba-1$^+$ (microglia/macrophages) immunoreactivity. (A) Representative images of the anti-Iba-1 immunoreactivity showing Iba-1$^+$ cells within the infarct, at the periphery of the infarct and in the contralateral striatum at both days 14 (n = 4/group) and 35 (n = 4/group) post ischemia for both control and PLX5622-treated mice. (B) A significantly decreased percentage of Iba-1$^+$ area within the infarct of PLX5622-treated mice compared to control mice at day 35 post ischemia was observed. Values are depicted as mean ± SEM (3 fields of view per region per mouse) (*$p < 0.05$, **$p < 0.01$, ***$p < 0.005$; * vs. treatment, # vs. time, & vs. infarct).

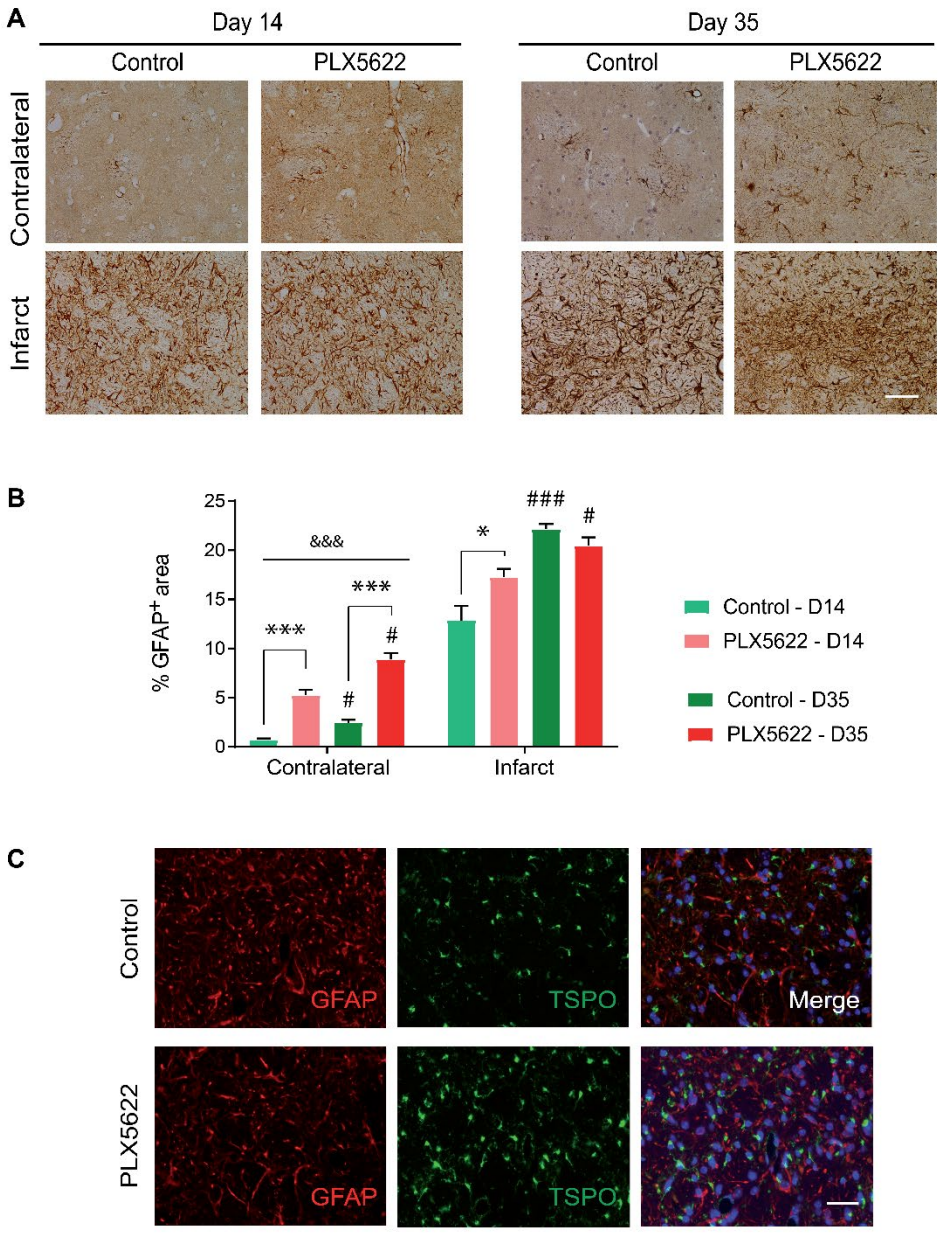

Supplementary Figure 7. Number of GFAP$^+$ increased over time after acute PLX5622 treatment. (A) Representative GFAP staining within the infarct and contralateral striatum for both experimental groups at days 14 and 35 post ischemia. (B) Treatment effect was observed in both regions at day 14: PLX5622-treated mice showed a higher percentage of GFAP$^+$ area compared to control mice in both infarct ($p = 0.014$) and contralateral striatum ($p < 0.001$). At day 35 post ischemia, treatment effect was still observed in the contralateral striatum while no difference was observed within the infarct. (C) No colocalization between GFAP and TSPO was observed at day 14 post ischemia, indicating that astrocytes were not

contributing to the increased 18F-DPA-714 PET signal in PLX5622-treated mice at day 14 post ischemia. Values are depicted as mean ± SEM (control: n = 4 and PLX5622: n = 4 for both time points, 3 fields of view per region per mouse, scale bar: 20 µm) (*$p < 0.05$, **$p < 0.01$, ***$p < 0.005$; * vs. treatment, # vs. time, & vs. infarct).

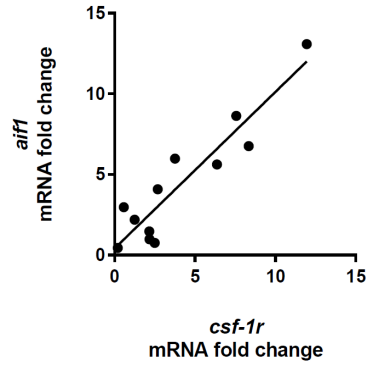

Supplementary Figure 8. Positive correlation between *aif1* and *csf-1r* gene expression during repopulation (R^2 = 0.86).

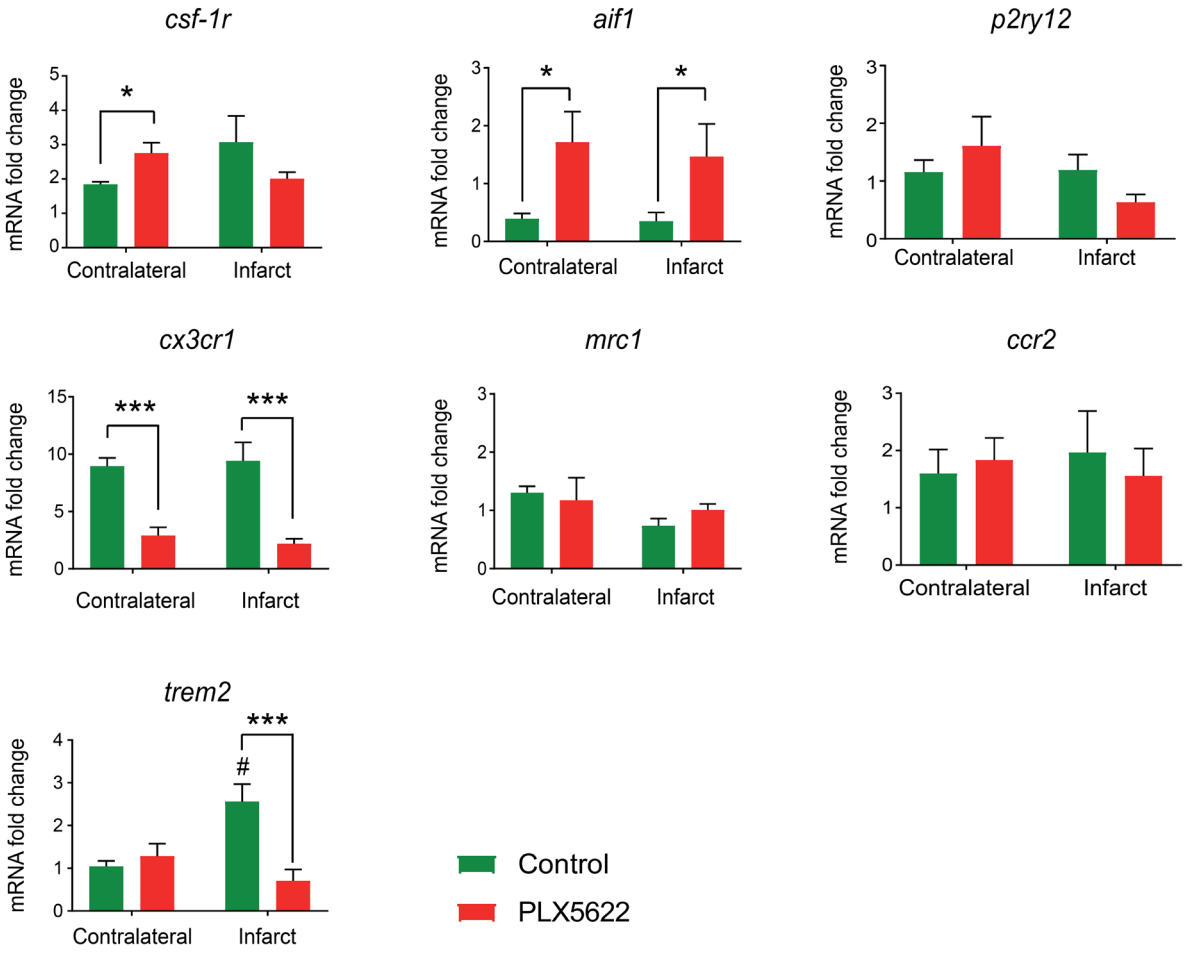

Supplementary Figure 9. Gene expression of microglia/macrophages-related markers at day 35 post ischemia (n = 4/group; *$p < 0.05$, **$p < 0.01$, ***$p < 0.005$, # vs contralateral).